A NOVEL METHOD FOR COMPUTING THE FULL-ENERGY PEAK EFFICIENCY OF COAXIAL HIGH-PURITY GERMANIUM DETECTORS FOR CYLINDRICAL SOURCES

D. GURAU[1], D. STANGA[1], L. DONE[1], O. SIMA[1,2], G. ILIE[3]

[1]*Horia Hulubei National Institute of R&D in Physics and Nuclear Engineering (IFIN-HH), 30 Reactorului, POB MG-6, Magurele, 077125, Romania*
[2]*University of Bucharest, Physics Department, Bucharest-Magurele, POB MG-12, Romania*
[3]*Mirion Technologies, 800 Research Parkway, Meriden, CT 06450, USA*
Corresponding author: doru@nipne.ro

Receipt date: 08 July 2024

Abstract. In this work a novel method for computing the full-energy peak efficiency of coaxial HPGe detectors for cylindrical sources emitting photons in the range of 60 - 2000 keV is described. It has a solid theoretical basis using an integral expression for computing the full-energy peak efficiency via computed values of the detector response and the attenuation factor of point sources. The method was implemented as a Matlab code written for computing the full-energy peak eficiency of a Canberra detector. The code was extensively verified by intercomparison with GESPECOR and LabSOCS codes and the results are fit purpose e.g. in the measurement of environmental samples.

Key words: gamma spectrometry, full-energy peak efficiency, computational method, Matlab code.

1. INTRODUCTION

Computed values of the full-energy peak (FEP) efficiency are widely used in gamma spectrometry measurements for determining the activity of gamma emitting sources because the relative method of measurement has severe restrictions [1]. Monte Carlo (MC) simulation models, implemented as computer codes, are often used for computing the FEP efficiency of gamma spectrometry systems. Before using MC simulation codes, the geometric model of the detector must be calibrated [2, 3]. Once calibrated, these codes can be used as reference codes for computing accurately the FEP efficiency with settled computational errors. However, MC simulation codes are rather complicated, time consuming and require skilled people for their use and the calibration of the detector model.

The deterministic methods, implemented as computer codes, are usually simpler and faster than MC simulation codes providing sufficiently accurate values of the FEP efficiency [4]. In many cases, the use of deterministic codes is more convenient for computing the FEP efficiency especially when the sample geometry is poorly known [5]. The deterministic methods are based on the integral expressions for computing the FEP efficiency, which make use of three probability functions [4]. Because analytical expressions cannot be developed for the probability function p_{fep} of detected photons to be registered in the FEP due to the complexity of the detection process, the deterministic methods make always use of approximations and simplifications [6]. Hybrid methods were also developed, which make use of both integral expressions for computing the FEP efficiency and MC simulation codes [7].

In this work a simple and fast method was developed to compute the FEP efficiency for cylindrical sources using a hybrid approach. It is based on an integral expression for computing the FEP efficiency of cylindrical sources via computing the FEP efficiency response of the detector and the attenuation factor of point sources embedded in the source matrix. The FEP efficiency response is computed using the grid based linear interpolation, while the FEP efficiency response in grid points is computed by means of a MC simulation code with a properly calibrated model of the detector. The attenuation factor is computed using MC integration and the FEP efficiency for cylindrical sources is computed according to the integral expression mentioned above using numerical integration. The method can be applied for computing the FEP efficiency of coaxial HPGe detectors for homogeneous cylindrical sources with uniform activity distribution placed coaxially with the detector axis and emitting photons in the 60 - 2000 keV range. The sources must be located inside the space bounded by a right circular cylinder (radius and length equal to 15 cm and 30 cm) placed on the detector end cap coaxially with the detector axis. This space can accommodate almost all sources measured by gamma spectrometry laboratories.

The novel method was implemented as a computer code using Matlab software [8]. It was applied to the computation of the FEP efficiency for cylindrical sources using a Canberra p-type coaxial HPGe detector, model GC3018. The Matlab code was extensively verified by intercomparison with GESPECOR [9] code in order to evaluate the intrinsic errors of the method. The results show that the Matlab code has sufficiently small intrinsic errors. The Matlab code was also verified by intercomparison with LabSOCS code, which is widely used by gamma spectrometry laboratories [10]. The results show that there is a good agreement between LabSOCS and Matlab codes.

2. THEORETICAL BASIS

Let us consider the gamma counting geometry shown schematically in Fig.1, where the detector is a coaxial HPGe detector and the sample is homogenous with the linear attenuation coefficient $\mu_s(E)$.

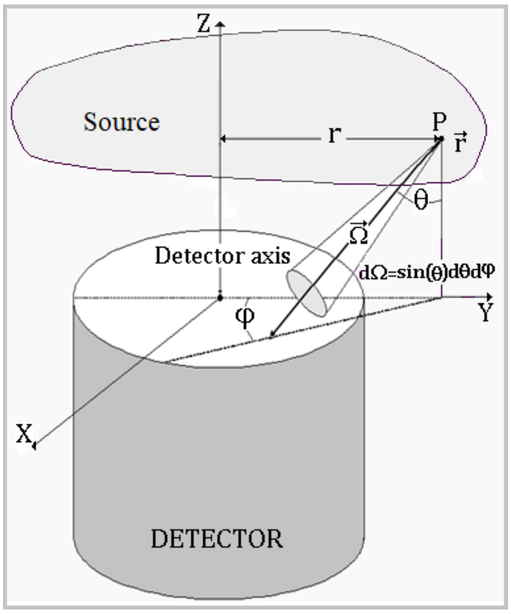

Fig. [1] - Schematic view of the configuration detector-volume source

For a point source P located inside the sample at the position $\vec{r}$ emitting photons of energy E in the direction $\vec{\Omega}$ defined by the angles θ and φ, the full-energy peak efficiency of the detector $\varepsilon_{pp}(\mu_s, E, \vec{r})$ [4,11,12] is given by:

$$\varepsilon_{pp}(\mu_s, E, \vec{r}) = \frac{1}{4\pi}\int_\Omega p_{pp}(\mu_s, E, \vec{r}, \vec{\Omega})d\Omega = \frac{1}{4\pi}\int_\Omega f_t(\vec{r}, \vec{\Omega})p_{pp}^o(E, \vec{r}, \vec{\Omega})\, d\Omega = \frac{\Omega}{4\pi}M_\Omega(p_{pp}) \quad (1)$$

where $\varepsilon_{pp}(\mu_s, E, \vec{r})$ is the FEP efficiency of the detector, $p_{pp}(\mu_s, E, \vec{r}, \vec{\Omega})$ is the probability of the photons of energy E emitted in the direction $\vec{\Omega}$ by the point source P to be detected and registered in the FEP, $p_{pp}^o(E, \vec{r}, \vec{\Omega})$ is the probability of detecting and registering the photons of energy E in the FEP in the absence of the attenuation (point source P placed in vacuum), $f_t(\vec{r}, \vec{\Omega})$ is the transmission factor of the photons through the sample material and absorbing layers interposed between the sample and the detector and $M_\Omega(p_{pp})$ is the integral mean of p_{pp} over the solid angle Ω subtended by the active volume of the crystal at the point source P (note that the first subscript in quantities like p_{pp} refers to the peak, while the second, to the point source). It should be emphasized that $p_{pp} = p_{tp}p_{fep}$, where p_{tp} represents the probability of detecting and counting the photons of energy E emitted in the direction $\vec{\Omega}$ by the point source P that did not interact with the sample material and the materials interposed between the detector and the sample and p_{fep} is the probability of detected photons to be registered in the FEP. The probability function p_{tp} can be expressed using elementary functions but the probability function p_{fep} cannot be expressed through elementary functions due to the complexity of the detection process of the gamma radiation. However, approximations of p_{fep} can be used for computing the FEP efficiency. A simple approximation consists of taking p_{fep} as a constant function for a given value of E, that is, $p_{fep}(E,\vec{r},\vec{\Omega}) = p_{fep}(E)$. This approximation is used by the efficiency transfer method based on the invariability of the peak-to-total ratio [4, 6].

According to Eq. (1), the FEP efficiency response of the detector for a point source placed in vacuum is given by [4]:

$$\varepsilon_{pp}^{o}(E,\vec{r}) = \frac{1}{4\pi}\int_{\Omega} p_{pp}^{o}(E,\vec{r},\vec{\Omega})d\Omega = \frac{\Omega}{4\pi}M_{\Omega}(p_{pp}^{o}) \quad (2)$$

where $M_{\Omega}(p_{pp}^{o})$ is the integral mean of p_{pp}^{o} over the solid angle Ω. Using Eq. (1) and Eq. (2) one obtains:

$$\varepsilon_{pp}(\mu_s,E,\vec{r}) = \frac{\Omega}{4\pi}M_{\Omega}(f_t p_{pp}^{o}) = M_{\Omega}(f_t)[1 + T_{\Omega}^{N}(f_t,p_{pp}^{o})]\varepsilon_{pp}^{o}(E,\vec{r}) = f_{at}\varepsilon_{pp}^{o} \quad (3)$$

where $f_{at}(\mu_s,E,\vec{r}) = \varepsilon_{pp}(\mu_s,E,\vec{r})/\varepsilon_{pp}^{o}(E,\vec{r})$ is the attenuation factor for the point source P embedded in the volume sample at the position $\vec{r}$, $T_{\Omega}^{N}(f_t,p_{pp}^{o}) = T_{\Omega}(f_t,p_{pp}^{o})/[M_{\Omega}(f_t)M_{\Omega}(p_{pp}^{o})]$ and $T_{\Omega}(f_t,p_{pp}^{o}) = M_{\Omega}\{[f_t - M_{\Omega}(f_t)][p_{pp}^{o} - M_{\Omega}(p_{pp}^{o})]\}$ is the Chebyshev functional. Assuming that the attenuation of the materials located between the sample matrix and the detector is negligible ($f_t \approx f_s$), it was proved that the values of $T_{\Omega}^{N}(f_t,p_{pp}^{o})$ are close to zero for small deviations of the transmission factor $f_t(\mu_s,\vec{r},\vec{\Omega})$ from its mean value [4]. These deviations are small for small deviations of $\mu_s l_s$ from its mean value and this happens when: (i) the values of μ_s are small, (ii) the deviations of l_s from its mean are small and (iii) both conditions (i) and (ii) are fulfilled. Under these conditions, it follows from Eq. (3) that:

$$f_{at}(\mu_s,\vec{r}) = M_{\Omega}(f_t) + R_f = \frac{1}{\Omega}\int_{\Omega} f_t(\mu_s,\vec{r},\theta,\varphi)\sin(\theta)\,d\theta d\varphi + R_f \quad (4)$$

where the remainder R_f term is small. It is evident that R_f is small for samples located far away (e.g., 50 cm) from the detector because the deviations of l_s from its mean are small in this case. Even for samples located in the close proximity of the detector (e.g. samples located on the detector end cap) R_f is small when μ_s is small (e.g. μ_s < 1.0 cm^{-1}) in the photon energy range of 60 - 2000 keV and this happens for the large majority of samples measured by gamma spectrometry laboratories.

For a sample with uniform activity distribution, the FEP efficiency, $\varepsilon_{ps}(\mu_s,E)$ (subscrip p denotes quantities referring to the peak, subscript s to the volume sample) of the detector [4] is given by:

$$\varepsilon_{ps}(\mu_s, E) = \frac{1}{V}\int_V \varepsilon_{pp}(\mu_s, E, \vec{r})dV = M_V(\varepsilon_{pp}) = M_V(f_{at}\varepsilon_{pp}^{o}) \quad (5)$$

where $M_V(\varepsilon_{pp})$ is the integral mean of ε_{pp} over the volume V of the sample. Eq. (5) can be computed by numerical integration using a set of point sources for which the FEP efficiency responses and the attenuation factors must be known. In this way, the direct use of the unknown probability function p_{fep} is avoided.

3. DESCRIPTION OF THE NOVEL METHOD

In this work, a novel method has been developed making use of the integral equation expressed by Eq. (5) and a MC simulation code. It can be applied to compute the FEP efficiency of coaxial HPGe detectors for homogeneous cylindrical sources with uniform activity distribution placed coaxially with the detector axis and emitting photons in the range of 60 - 2000 keV. The cylindrical sources must be located inside the space bounded by a right circular cylinder placed on the detector end cap coaxially with the detector axis.

In order to compute the FEP efficiency for cylindrical samples according to Eq. (5), the FEP efficiency responses of the detector (for point sources placed in vacuum) were determined using a grid based interpolation technique and the attenuation factors for point sources embedded in the source matrix were computed using MC integration. At the end, the FEP efficiency for cylindrical samples was computed according to Eq. (5) using numerical integration (midpoint rule).

3.1. COMPUTING THE FEP EFFICIENCY RESPONSE OF THE DETECTOR USING GRID BASED INTERPOLATION

The interpolation of gridded data is more efficient than the interpolation of scattered data due to the organized structure of the gridded data. This is the reason that the grid based interpolation must be used, whenever possible [7].

In order to compute the FEP efficiency response of coaxial HPGe detectors using the grid based interpolation, a 3D grid must firstly be created taking account that the FEP efficiency response depends on the photon energy E, the radial cylindrical coordinate r and the axial cylindrical coordinate z. The coordinates r and z are defined relative to the coordinate system with the origin located at the center of the entrance surface of the detector end cap and its longitudinal axis is coincident with the detector axis. Hence, the 3D grid is defined by the following grid vectors: $r = (r_1, r_2, \dots, r_m = r_{max})$, $z = (z_1, z_2, \dots, z_n = z_{max})$ and $E = (E_1, E_2, \dots, E_l)$, where r_1 = z_1 = 0, E_1 = 60 keV and E_l= 2000 keV. The values of these vectors must be strictly monotonic. As one can see, for a given photon energy, the spatial grids are created in (r, z) space above the detector corresponding to the space bounded by a right circular cylinder placed on the detector end cap coaxially with the detector axis that has the height and radius equal to z_{max} and r_{max}, respectively. This space for z_{max}= 30 cm and r_{max}= 15 cm can accommodate almost all cylindrical samples measured by gamma spectrometry laboratories.

The values of the FEP efficiency response in grid points can be computed using a MC simulation code provided with a properly calibrated geometric model of the coaxial HPGe detector. Then, a grid based interpolation method must be employed to compute $\varepsilon_{pp}^{o}(E,r,z)$ at any values of r, z and E using its computed values in grid points. In this work, GESPECOR code with a properly calibrated model of the detector was used for computing ε_{pp}^{o} in grid points [2]. The interpolating function *interpn* from Matlab software was used to compute ε_{pp}^{o} by linear interpolation at specified values of r, z and E located between grid points employing linear interpolation. This method of interpolation has the advantage of being fast and may provide accurate results when the values of grid vectors are closely spaced.

3.2 COMPUTING THE ATTENUATION FACTORS OF POINT SOURCES EMBEDDED IN THE SOURCE MATRIX

The attenuation factors of point sources were computed approximately by means of Eq. (4) using MC integration and taking R_f= 0. Thus, a large number N of pairs of angles (θ_i,φ_i) were generated randomly in the solid angle Ω subtended by the active volume of the crystal at the point source and the transmission factor was determined for each pair of angles. According to Eq. (4), the attenuation factor for a point source located at the position (r,z) is given by:

$$f_{at}(r,z)=\frac{1}{N}\sum_{i=1}^{N}f_t(r,z,\theta_i,\varphi_i) \tag{6}$$

Let us consider the longitudinal section through the cylindrical source-detector configuration shown in Fig.2. The transmission factor for a point source placed inside the cylindrical source at the position (r,z) is given by:

$$f_t=\exp(-\mu_s l_s-\mu_c l_c) \tag{7}$$

where l_s is the path length traversed by photons through the sample matrix, μ_c is the linear attenuation coefficient of the container material and l_c is the path length traversed by photons through the base or wall of the container.

For large cylindrical sources having $R_s > R_D$ with R_D the radius of the active volume of the detector (see Fig.2a), the photons emitted by the source in the solid angle Ω emerge always from source through the base of the source matrix and the container. Consequently, $l_s=h_s/\cos(\theta)$ and $l_c=t_{cb}/\cos(\theta)$. Note that if $r > R_D$ the range of φ angles from the solid angle is limited, whereas if $r < R_D$ there is no limitation in the range of the φ angles. For small cylindrical sources with $R_s < R_D$ (see Fig. 2b), the photons emitted by the source in the solid angle Ω emerge from source either through the base or the side face of the source matrix and the container.

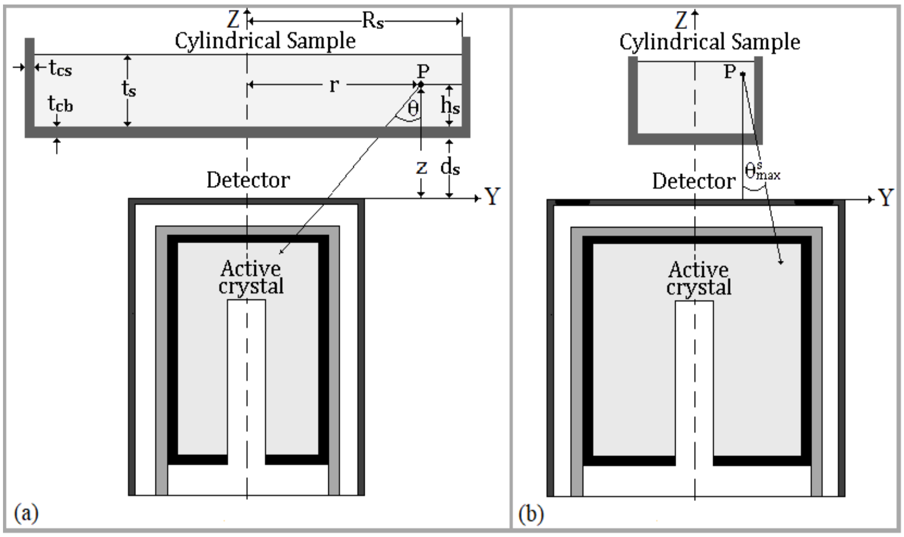

Fig. [2] - Longitudinal section through the detector and the cylindrical source: (a) cylindrical source with the radius larger than the radius of the active volume of the detector; (b) cylindrical source with the radius smaller than the radius of the active volume of the detector

The two cases are defined in function of the angle $\theta_{max}^{s} = atan\left\{\left[r \cdot \cos(\varphi) + \sqrt{R_s^2 - r^2 \cdot sin^2(\varphi)}\right]/h_s\right\}$, which is the angle of incidence on the matrix base of the photon trajectory that links the emission point with the intersection point between the edge of the matrix base and the vertical plane rotated by φ with respect to the plane defined by the emission point and the detector axis. If $\theta \leq \theta_{max}^{s}$ then the photons emitted by the point source in the solid angle Ω emerge from the base of the matrix and container. In this case, $l_s = h_s/\cos(\theta)$ and $l_c = t_{cb}/\cos(\theta)$. If $\theta > \theta_{max}^{s}$, then the photons emerge from the source through the side face of the matrix and container and as such the path length l_s is given by $l_s = \left[rcos(\varphi) + \sqrt{R_s^2 - r^2 sin^2(\varphi)}\right]/\sin(\theta)$ and l_c can be expressed as $l_c = \left[\sqrt{(R_s + t_{cs})^2 - r^2 sin^2(\varphi)} - \sqrt{R_s^2 - r^2 sin^2(\varphi)}\right]/\sin(\theta)$.

3.3. COMPUTING THE FEP EFFICIENCY

The FEP efficiency ε_{ps} for a cylindrical sample was computed by numerical integration (midpoint rule) using Eq. (5). For a cylindrical sample, Eq. (5) becomes:

$$\varepsilon_{ps}(\mu_s, E) = \frac{1}{\pi R_s^2 t_s} \int_0^{R_s} \int_{z_{min}}^{z_{max}} \int_0^{2\pi} f_{at} \varepsilon_{pp}^{o} \, rdrdzd\varphi = \int_0^1 \int_0^1 f_{at} \varepsilon_{pp}^{o} \, dudq \quad (8)$$

where $u = (r/R_s)^2$, $q = (z - z_{min})/(z_{max} - z_{min}) = (z - z_{min})/t_s$, $z_{min} = d_s + t_{cb}$ and $z_{max} = z_{min} + t_s$ (see Fig. 2). Using the midpoint rule, ε_{ps} can be expressed as:

$$\varepsilon_{ps}(\mu_s, E) = \frac{1}{n_r n_h} \sum_{i=1}^{n_r} \sum_{j=1}^{n_z} f_{at}(r_i, z_j) \varepsilon_{pp}^{o}(r_i, z_j) + R_\varepsilon \tag{9}$$

where $r_i = R_s\sqrt{(i-0.5)/n_r}$, $z_j = z_{min} + (j - 0.5)(t_s/n_h)$, n_r and n_z are natural numbers. If n_r and n_z are sufficiently large then the remainder R_ε term is negligibly small. Using the linear index $k = (j-1)n_r + i$, Eq. (9) becomes:

$$\varepsilon_{ps}(\mu_s, E) = \frac{1}{M} \sum_{k=1}^{M} f_{at}(k) \varepsilon_{pp}^{o}(k) + R_\varepsilon \tag{10}$$

where $f_{at}(k) = f_{at}(r_i, z_j)$, $\varepsilon_{pp}(k) = \varepsilon_{pp}(r_i, z_j)$ and $M = n_r n_z$.

4. EVALUATION OF COMPUTATIONAL ERRORS

The FEP efficiency of coaxial HPGe detectors for homogeneous cylindrical sources with uniform activity distribution depends on the vector $X = (E, \mu_s, \mu_c, R_s, t_s, d_s, t_{cb}, t_{cs})$, assuming that the radius of the source matrix is equal to the inner radius of the source container (see Fig. 2). Generally, the FEP efficiency depends weakly on μ_c, t_{cb} and t_{cs}. It should be noted that μ_s and μ_c depend not only on E but also on the source matrix and the material of source container, respectively. In practice, discrete values of the FEP efficiency for a given vector X can be obtained by measurement or computation.

All computer models (including deterministic methods) of computing the FEP efficiency are always subject to computational errors because they make always use of approximations and simplifications. Taking these errors into account, $\varepsilon_i^{true} = \varepsilon^{true}(X_i)$ can be written as:

$$\varepsilon_i^{true} = \varepsilon_i^{c} + \Delta_i \tag{11}$$

where $\varepsilon_i^{c} = \varepsilon^{c}(X_i)$ denotes the computed value of the FEP efficiency corresponding to the vector X_i and $\Delta_i = \Delta(X_i)$ is the discrepancy between ε_i^{true} and ε_i^{c}, which represents the computational error of the model. Because ε_i^{true} is unknown, in order to get information on the computational errors, ε_i^{true} is replaced by reference values of the FEP efficiency, which are usually the measured values of the FEP efficiency. Let $\varepsilon = \{\varepsilon_1, \varepsilon_2, \ldots\ldots, \varepsilon_n\}$ be a set of reference values of the FEP efficiency corresponding to the set of vectors $\{X_1, X_2, \ldots\ldots, X_n\}$ (e.g. FEP efficiency values corresponding to different source positions and photon energies). To incorporate the randomness of these value, the following equation is used:

$$\varepsilon_i = \varepsilon_i^{true} + e_i \tag{12}$$

where $\{e_i\}_1^n$ is a set of independent random variables (measurement errors) with assumed zero mean and possibly unequal variances. In gamma spectrometry measurements, usually e_i follows a normal distribution $N(0, \sigma_i^2)$, where $\sigma_i^2 = var(\varepsilon_i)$ is the variance of ε_i. Generally, the standard deviations σ_i may vary much in gamma spectrometry measurements but the relative standard deviations σ_i/ε_i are not much different ranging customarily from 2 % to 5 %. From Eq. (11) and Eq. (12), one obtains the following equation:

$$\varepsilon_i = \varepsilon_i^c + \Delta_i + e_i \tag{13}$$

Eq. (13) represents the statistical model that allows the evaluation of computational errors, i.e. Δ_i. Using the relative discrepancy defined by $\delta(\Delta_i) = \Delta_i/\varepsilon_i^c$, Eq. (15) can be rewritten as follows:

$$\delta(\varepsilon_i^c) = \delta(\Delta_i) + \delta(e_i) \tag{14}$$

where $\delta(\varepsilon_i^c) = (\varepsilon_i - \varepsilon_i^c)/\varepsilon_i^c$ is the relative deviation (RD) of ε_i^c from ε_i and $\delta(e_i) = e_i/\varepsilon_i^c$ is approximatively the relative measurement error (ε_i^c is close to ε_i). Notice that for each i $\delta(e_i)$ follows a normal distribution $N[0, (\sigma_i/\varepsilon_i^c)^2]$, where $(\sigma_i/\varepsilon_i^c)^2 = var[\delta(e_i)]$. As one can see from Eq. (14), the relative discrepancy $\delta(\Delta_i)$ may differ significantly from $\delta(\varepsilon_i^c)$ when the absolute value (modulus) of the relative measurement error is large. However, an upper limit for the absolute value of the relative discrepancy $|\delta(\Delta_i)|$ can be estimated from Eq. (14). Thus, the following inequality can be derived:

$$|\delta(\Delta_i)| < |\delta(\varepsilon_i^c)| + \delta^{max}(e_i) \tag{15}$$

where $\delta^{max}(e_i) = 2(\sigma_i/\varepsilon_i^c)$ can be taken approximately as an upper limit for $\delta(e_i)$. The above inequality shows that $|\delta(\varepsilon_i^c)|$ is approximately an upper limit for $|\delta(\Delta_i)|$ only when $|\delta^{max}(e_i)|$ is significantly smaller than $|\delta(\varepsilon_i^c)|$. This means that high accuracy standard sources are required for measuring accurately the reference values of the FEP efficiency and determining approximately upper limits for the relative discrepancy.

The mean value of the data set $\{\delta(\Delta_1), \delta(\Delta_2), \dots, \delta(\Delta_n)\}$ is given by $\bar{\delta}(\Delta) = (1/n)\sum_1^n \delta(\Delta_i)$. From Eq. (14), it follows that:

$$\bar{\delta}(\Delta) = \bar{\delta}(\varepsilon^c) + R_{av} \tag{16}$$

where $\bar{\delta}(\varepsilon^c) = (1/n)\sum_1^n \delta(\varepsilon_i^c)$ and the remainder term $R_{av} = \bar{\delta}(e) = (1/n)\sum_1^n \delta(e_i)$. According to the weak law of large numbers, R_{av} converge in probability to zero when n goes to infinity. Also, taking into account that $\delta(e_i)$ follows a normal distribution with zero mean, then for any $t > 0$ the following inequality [13] holds:

$$P\left[\left|\bar{\delta}(e_i)\right| \le t\right] \ge 1 - 2\exp[-0.5(t^2/\sigma^2)] = 1 - 2\exp[-0.5n(t^2/\sigma_m^2)]$$

(17)

where $\sigma^2 = var[\bar{\delta}(e)] = (1/n^2)\sum_1^n(\sigma_i/\varepsilon_i^c)^2 = \sigma_m^2/n$ and $\sigma_m^2 = (1/n)\sum_1^n(\sigma_i/\varepsilon_i^c)^2$. The above inequality shows that the probability $P[|\bar{\delta}(e)| \leq t]$ is high (e.g. higher than 0.95) when n takes sufficiently large values even if t is very close to zero. For example, if t = $0.25\sigma_m$= 0.005 and $P[|\bar{\delta}(e)| \leq 0.005]$ = 0.95, then n = 118. This shows that a large number of cylindrical sources must be measured for determining $\bar{\delta}(\Delta)$ accurately.

As it was shown above, the evaluation of computational errors by means of measured values of the FEP efficiency is not only difficult but also laborious because a large number of sources must be measured accurately. One way of alleviating this burden is based on the use of computed values of the FEP efficiency provided by a MC simulation code with a pre-calibrated model of the detector. In this case, Eq. (14) can be written as:

$$\delta_{mc}(\varepsilon_i^c) = \delta(\Delta_i) + \delta(e_i^{mc}) \tag{18}$$

where $\delta_{mc}(\varepsilon_i^c) = (\varepsilon_i^{mc} - \varepsilon_i^c)/\varepsilon_i^c$, ε_i^{mc} is the reference value of the FEP efficiency computed by means of the MC simulation code and e_i^{mc} is the relative computational error of the code. In case that only a maximum value of computational errors is known, then the upper limit of the absolute value of the relative discrepancy is given by $|\delta(\Delta_i)| < |\delta_{mc}(\varepsilon_i^c)| + \delta^{max}$, where δ^{max} is the maximum value of $|\delta(e_i^{mc})|$ when i = 1,2,...,n.

The mean values and the maximum (upper limit) of the absolute values of the relative deviations can be used as indicators of the quality of computational results [14]. If these mean and maximum values are sufficiently small, then the computational results are sufficiently accurate and can be accepted as satisfactory results.

5. RESULTS

5.1. APPLICATION OF THE NOVEL METHOD

The novel method was applied to a p-type coaxial HPGe detector, which is a Canberra detector model GC3018 with the relative FEP efficiency of 34 % and the resolution (FWHM) of 1.73 keV at 1.33 MeV. To generate the 3D grid, the GESPECOR code was used to compute the FEP efficiency response ε_{pp}^o of the detector in grid points. To obtain accurate values of the FEP efficiency response in grid points, the GESPECOR model of the HPGe detector GC3018 was previously calibrated [2]. The 3D grid was defined by the following grid vectors: r_g (cm) = [0, 0.5, 1, 1.5, 2, 2.5, 3, 3.5, 4, 5, 6, 8, 10, 12, 14, 15]; z_g (cm) = [0, 0.25, 0.5, 0.75, 1, 1.5, 2, 2.5, 3, 4, 5, 7, 9, 11, 13, 15, 17, 19, 21, 23, 25, 27, 28, 29, 30]; $E_g\ (keV)$ = [60, 70, 80, 100, 125, 150, 200, 250, 300, 350, 400, 500, 600, 750, 900, 1000, 1100, 1300, 1450, 1600, 1800, 2000].

The novel method was implemented as a computer code using Matlab software. A first Matlab function was written for computing the FEP efficiency response between grid points using linear interpolation. A second Matlab function was written for computing the attenuation factors as it was described before in section 3.2. Using these two functions, a Matlab code was developed for computing the FEP efficiency for cylindrical sources as it was described in section 3.3.

5.2 VERIFICATION OF THE METHOD USING GESPECOR CODE

The intrinsic errors of the Matlab code are due to the grid-based interpolation, the approximations used for computing the attenuation factors and the numerical integration (midpoint rule) of Eq. (5). These errors were evaluated by means of GESPECOR code that is free of these errors and it was used for computing the FEP efficiency response of the detector in grid points. Consequently, the Matlab code was extensively verified using several cylindrical sources, which emit a large number of gamma-lines and are placed coaxially with the detector axis at different positions relative to the detector. The container of all sources is made of plastic (PVC) with thickness of the base and the wall equal to 0.1 cm. To this aim, the FEP efficiency of the coaxial HPGe detector type GC3018 for a given cylindrical source was computed using GESPECOR and Matlab codes and the relative deviation between their results was calculated as it was described in section 4. Thus, the values of the FEP efficiency for cylindrical sources belonging to the set $S = M \times R_s \times t_s \times d_s \times E$, where $M = \{Water, Al\}$, $R_s(cm)$ = {1, 10}, $t_s(cm)$ = {1, 3, 5}, $d_s(cm)$ = {0, 5} and $E(keV)$={60, 80, 100, 120, 150, 200, 300, 600, 1250, 1500, 2000}. Each element of the set S is a 5-tuple representing a cylindrical source whose matrix is either water or aluminum and which has specified values for R_s and t_s being placed at a given distance d_s from the detector end cap and emitting a single gamma-line. Hence, the set S contains 264 points (5-tuples) in 5D space corresponding to 264 sources (each of them emitting only one gamma-line).

Table 1 shows the relative deviations between GESPECOR and Matlab codes for sources belonging to the set S. In other words, the relative deviations in Table 1 were calculated for cylindrical sources placed at the distances 0.0 cm and 5.0 cm from the detector end cap, which have the matrix of water and aluminum with $R_s(cm) \in \{0.5, 1.5\}$ and $t_s(cm) \in \{1, 3, 5\}$ and emit the gamma-lines belonging to the set E. The mean value of the relative deviations from Table 1 is equal to 0.55 % and their maximum absolute value is 5.35 %.

It should be mentioned that the relative deviations between GESPECOR and Matlab codes may take significantly higher values than the maximum absolute value of the relative deviations shown in Table 1 (5.35 %). This happens for cylindrical sources that emit low energy photons (e.g. $E < 130$ keV) having the value of the energy located between grid points and is due to interpolation errors with respect to photon energy. For illustration, in Table 2 are shown the relative deviations for cylindrical sources from the set $S_1 = M \times R_s \times t_s \times d_s \times E_1$, where the set E_1={65, 75, 90, 110,130} contains the values of the energy located between grid points.

Table 1

Computed values of the relative deviations between GESPECOR and Matlab codes for cylindrical sources belonging to the set S (see the text)

d_s (cm)	E (keV)	Source matrix: water						Source matrix: aluminum					
		R_s=1 cm			R_s=10 cm			R_s=1 cm			R_s=10 cm		
		t_s (cm)			t_s (cm)			t_s (cm)			t_s (cm)		
		1	3	5	1	3	5	1	3	5	1	3	5
0	60	1.19	0.01	-0.67	3.43	2.46	1.66	1.82	-1.72	-3.55	5.35	4.00	3.56
	80	0.71	-0.32	-0.94	2.18	1.45	0.94	0.79	-1.99	-3.59	3.13	2.03	1.49
	100	0.59	-0.50	-1.19	1.69	1.13	0.79	0.55	-2.14	-3.65	2.26	1.41	0.96
	120	1.46	0.18	-0.59	2.36	1.98	1.85	1.53	-1.35	-2.99	2.95	2.37	2.20
	150	0.70	-0.67	-1.53	1.39	1.17	1.07	0.72	-2.35	-4.17	1.84	1.48	1.31
	200	0.78	-0.72	-1.67	1.38	1.31	1.27	0.90	-2.40	-4.37	1.86	1.73	1.67
	300	0.83	-0.64	-1.70	1.34	1.46	1.48	1.02	-2.28	-4.47	1.80	1.99	2.02
	600	0.83	-0.51	-1.39	1.25	1.35	1.43	1.05	-1.92	-3.87	1.75	1.98	2.10
	1250	0.66	-0.33	-0.98	1.24	1.48	1.26	0.85	-1.41	-2.98	1.65	2.07	1.89
	1500	0.69	-0.25	-0.85	1.23	1.30	1.28	0.87	-1.22	-2.71	1.63	1.87	1.90
	2000	0.25	-0.55	-1.14	0.58	0.85	0.97	0.41	-1.44	-2.83	0.96	1.40	1.57
5	60	2.07	1.86	1.25	0.68	0.27	0.04	1.68	-0.12	-2.21	0.14	-0.53	-0.72
	80	1.86	1.43	0.73	0.71	0.35	0.16	1.56	-0.09	-1.94	0.41	-0.16	-0.38
	100	1.77	1.27	0.52	0.77	0.51	0.36	1.53	-0.11	-1.89	0.61	0.21	0.05
	120	2.26	1.76	0.96	1.57	1.35	1.29	2.11	0.66	-1.21	1.54	1.35	1.32
	150	1.60	1.06	0.25	0.90	0.76	0.69	1.44	-0.11	-1.99	0.89	0.74	0.67
	200	1.50	0.98	0.10	0.95	0.85	0.78	1.37	-0.11	-2.08	1.01	0.96	0.92
	300	1.45	0.93	0.08	0.99	0.96	0.93	1.34	-0.14	-2.06	1.09	1.14	1.12
	600	1.33	0.86	0.15	1.06	1.06	1.05	1.26	0.00	-1.71	1.17	1.29	1.32
	1250	1.29	0.89	0.35	1.23	1.19	0.96	1.24	0.28	-1.05	1.33	1.40	1.22
	1500	1.19	0.77	0.27	1.10	1.09	1.00	1.14	0.19	-1.02	1.19	1.29	1.26
	2000	1.02	0.54	0.02	0.84	0.81	0.75	0.98	0.02	-1.16	0.93	0.99	0.98

The mean value of the relative deviations from Table 2 is equal to 2.30 % and their maximum absolute value is 8.61 %. As one can see, these values are significantly higher than the values corresponding to Table 1.

Table 2

Computed values of the relative deviations between GESPECOR and Matlab codes for cylindrical sources belonging to the sets S_1 that emit low energy photons and have the values of the energy located between grid points

d_s (cm)	E (keV)	Source matrix: water						Source matrix: aluminum					
		R_s=1 cm			R_s=10 cm			R_s=1 cm			R_s=10 cm		
		t_s (cm)			t_s (cm)			t_s (cm)			t_s (cm)		
		1	3	5	1	3	5	1	3	5	1	3	5
0	65	4.47	3.12	2.38	7.35	6.34	5.55	5.19	2.02	0.16	8.61	7.55	7.14
	75	2.37	1.19	0.53	4.67	3.71	3.04	2.71	-0.12	-1.85	5.22	4.26	3.83
	90	3.05	1.78	1.04	5.51	4.41	3.80	3.10	0.16	-1.44	5.39	4.28	3.83
	110	1.99	0.76	-0.05	3.96	2.87	2.45	2.10	-0.67	-2.35	3.68	2.99	2.70
	130	1.06	-0.24	-1.03	2.73	1.77	1.41	1.10	-1.84	-3.54	2.21	1.69	1.41
5	65	4.37	4.09	3.51	4.20	3.66	3.40	4.23	2.75	0.95	4.00	3.56	3.52
	75	3.01	2.65	1.95	2.29	1.83	1.64	2.83	1.29	-0.51	2.07	1.60	1.55
	90	3.42	2.96	2.24	3.13	2.69	2.48	3.18	1.56	-0.26	2.86	2.27	2.07
	110	2.69	2.19	1.39	2.17	1.87	1.74	2.56	1.11	-0.69	2.13	1.90	1.87
	130	1.92	1.40	0.62	1.31	1.13	1.01	1.77	0.20	-1.61	1.26	1.10	1.01

One can conclude that Matlab code provides sufficiently accurate results for cylindrical sources because both the mean and maximum absolute value of relative deviations between GESPECOR and Matlab are sufficiently small, not exceeding 2.30 % and 8.61 %, respectively. For photon energies higher than about 150 keV, the mean and the maximum absolute values of the relative deviations are smaller that 0.47 % and 2.1 %, respectively.

5.3 VERIFICATION OF THE METHOD USING LABSOCS CODE

The Matlab code was also verified extensively by intercomparison with LabSOCS code, which is widely used by gamma spectrometry laboratories for computing with sufficient accuracy the FEP efficiency for a large variety of sources [10]. In this case, the FEP efficiency of the coaxial HPGe detector type GC3018 for cylindrical sources was computed using LabSOCS and Matlab codes. The relative deviations between LabSOCS and Matlab codes were determined for the same cylindrical sources mentioned above, which belong to the set S. The same container like that one described above was used for all sources. Table 3 shows the relative deviations between LabSOCS and Matlab codes.

As one can see in Table 3, the mean value of the relative deviations is equal to 1.69 % and their maximum absolute value is 5.49 %. One can conclude that there is a good agreement between the results provided by LabSOCS and Matlab codes.

Table 3

Computed values of the relative deviations between LabSOCS and Matlab codes for cylindrical sources belonging to the set S (see the text)

d_s (cm)	E (keV)	Source matrix: water						Source matrix: aluminum					
		R_s=1 cm			R_s=10 cm			R_s=1 cm			R_s=10 cm		
		t_s (cm)			t_s (cm)			t_s (cm)			t_s (cm)		
		1	3	5	1	3	5	1	3	5	1	3	5
0	60	4.80	3.10	2.31	2.87	2.44	1.76	5.49	1.29	-1.23	5.14	4.13	3.54
	80	4.44	3.02	2.41	2.19	1.83	1.44	4.65	1.34	-0.84	3.35	2.54	1.93
	100	4.25	2.85	2.21	1.80	1.53	1.29	4.38	1.30	-0.69	2.61	2.09	1.61
	120	4.65	3.22	2.60	2.26	2.12	2.07	4.84	1.78	-0.24	3.03	2.69	2.46
	150	2.73	1.43	0.78	0.18	0.19	0.16	2.85	-0.14	-2.21	0.77	0.63	0.39
	200	3.03	1.68	1.02	0.44	0.54	0.53	3.20	0.25	-1.88	1.03	1.06	0.94
	300	3.81	2.59	1.91	1.45	1.61	1.64	4.00	1.25	-0.89	1.99	2.20	2.13
	600	3.27	2.27	1.67	1.49	1.80	1.90	3.46	1.15	-0.76	2.03	2.45	2.50
	1250	3.76	2.99	2.55	1.82	1.93	1.75	3.93	2.13	0.57	2.28	2.56	2.38
	1500	2.32	1.69	1.39	1.25	1.29	1.20	2.48	0.90	-0.51	1.68	1.89	1.80
	2000	1.75	1.35	1.14	1.07	1.15	1.12	1.89	0.61	-0.59	1.47	1.71	1.70
5	60	3.64	3.48	2.94	1.58	0.32	0.86	3.37	1.77	-0.57	1.04	0.32	0.05
	80	3.57	3.27	2.66	1.52	0.66	1.02	3.33	1.88	-0.22	1.23	0.66	0.38
	100	3.50	3.07	2.40	1.44	0.97	1.06	3.35	1.90	-0.14	1.33	0.97	0.77
	120	3.83	3.36	2.64	1.93	1.75	1.71	3.72	2.39	0.29	1.91	1.75	1.64
	150	2.38	1.92	1.23	0.29	0.12	0.10	2.25	0.87	-1.19	0.28	0.12	-0.04
	200	2.30	1.85	1.13	0.45	0.40	0.23	2.20	0.88	-1.17	0.50	0.40	0.26
	300	2.95	2.69	2.04	1.44	1.51	1.29	2.87	1.75	-0.16	1.52	1.51	1.36
	600	2.63	2.47	2.02	1.72	1.83	1.63	2.57	1.71	0.10	1.81	1.83	1.78
	1250	2.92	2.50	2.03	1.87	1.84	1.36	2.88	1.98	0.58	1.97	1.84	1.53
	1500	2.31	1.95	1.48	1.10	1.03	0.69	2.27	1.45	0.13	1.18	1.03	0.84
	2000	2.26	1.71	1.22	0.92	0.92	0.65	2.23	1.26	-0.03	0.99	0.92	0.79

6. CONCLUSIONS

In this work, a novel method was developed that is useful for laboratory gamma spectrometry measurements of cylindrical sources. The method is fast and simple. It is simple because the user can focus solely on constructing an accurate model of the measurement configuration (e.g. radius and thickness of the source matrix, parameters of the container, distance between source and detector end cap) and no longer needs to be concerned with the detector itself. The method has a solid theoretical basis making use of an integral expression to compute the FEP efficiency of HPGe detectors for cylindrical sources via computed values of the FEP efficiency response of the detector and the attenuation factor of point sources embedded in the matrix of the source.

The FEP efficiency responses were computed using a grid based interpolation technique and their values in grid points were computed by means of a MC simulation code having the geometric model of the detector properly calibrated. It follows that these values of the FEP efficiency responses are valid only for a single detector for which the geometric model was calibrated obtaining in this way the optimal values of the detector parameters. Hence, the method cannot be extended to different detectors and this is its main limitation. However, the method can be applied to another detector but a new 3D grid must be created that must be appropriate to that detector. The attenuation factors of point sources were computed approximately using MC integration and evaluating the transmission factors corresponding to that point sources. The FEP efficiency for a cylindrical sample was computed by numerical integration (midpoint rule) according to the integral equation mentioned above using a large set of point sources.

The novel method was applied using the GESPECOR software for creating an appropriate 3D grid for a p-type coaxial HPGe detector, which is a Canberra detector model GC3018. The method was implemented as a computer code using the Matlab software. The Matlab code was extensively verified by intercomparison with GESPECOR code in order to evaluate the intrinsic errors of the method. The results showed that the Matlab code has sufficiently small intrinsic errors because the average and the maximum absolute values of the relative deviations between GESPECOR and Matlab codes don't exceed 2.30 % and 8.61 %, respectively. The Matlab code was also verified by intercomparison with LabSOCS code. The results showed that the average and the maximum absolute values of the relative deviations between LabSOCS and Matlab codes don't exceed 1.69 % and 5.49 %, respectively.

One can conclude that the novel method provides sufficiently accurate results. It is evident that it can be improved by reducing the interpolation errors and using better approximations for computing the attenuation factors. Also, the method can be extended to other shapes of sources provided that suitable integration methods and appropriate ray-tracing algorithms for determining the path length of photons through the sample are used.

Acknowledgments. This work was supported by NUCLEU Program within the National Research Development and Innovation Plan 2022-2027, carried out with the support of Management Center of Research, Development and Innovation (CMCDI), project code PN 23-21.

References

[1] O. Sima and D. Arnold, On the Monte Carlo simulation of HPGe gamma-spectrometry systems, *Applied Radiation and Isotopes* **67**, 701–705 (2009).

[2] D. Gurau, D. Stanga, L. Done, O. Sima, G. Ilie, Calibrating GESPECOR model of computing the full-energy peak efficiency of coaxial high-purity germanium detectors by Monte Carlo simulation, *Applied Radiation and Isotopes* **204**, 111135 (2024).

[3] D. Gurau, D. Stanga, L. Done, O. Sima, E. Ionescu, Computational Characterization of coaxial HPGe detectors using Monte Carlo simulation and nonlinear least squares optimization, *Romanian Reports in Physics* **75**, 806 (2023).

[4] D. Stanga and D.Gurau, Novel integral expressions for computing the full energy peak efficiency of gamma spectrometry systems, *Applied Radiation and Isotopes* **172**, 109689 (2021).

[5] T. Frosio, N. Menaa, P. Bertreix, M. Rimlinger, C. Theis, A novel technique for the optimization and reduction of gamma spectroscopy geometry uncertainties, *Applied Radiation and Isotopes* **156**, 108953 (2020).

[6] L. Moens, J. De Donder, L. Xi-lei, F. De Corte, A. De Wispelaere, A. Simonits, J. Hoste, Calculation of the absolute peak efficiency of gamma-ray detectors for different counting geometries, *Nuclear Instruments and Methods in Physics Research* **187**, 451–472 (1981).

[7] R. Venkataraman, F. Bronson, V. Atrashkevich, M. Field, B. M. Young, Improved detector response characterization method in ISOCS and LabSOCS, *Journal of Radioanalytical and Nuclear Chemistry* **264** (1), 213-219 (2005).

[8] Matlab software, Natick, Massachusetts: MathWorks Inc., https://www. mathworks.com.

[9] O. Sima, D. Arnold, C. Dovlete, GESPECOR: A versatile tool in gamma-ray spectrometry, *Journal of Radioanalytical and Nuclear Chemistry* **248** (2), 359–364 (2001).

[10] P. J. LeBlanc, F. Bronson, W. F. Mueller, W. Russ, R. Venkataraman, Mathematical efficiency calibration methods for high quality laboratory based gamma spectrometry systems, *Journal of Radioanalytical and Nuclear Chemistry* **296**, 1045–1049 (2013).

[11] M. Barrera, A. Suarez-Llorens, M. Casas-Ruiz, J. J. Alonso, J. Vidal, Theoretical determination of gamma spectrometry systems efficiency based on probability functions. Application to self-attenuation correction factors, *Nuclear Instruments and Methods in Physics Research A* **854**, 31–39 (2017).

[12] O. Sima, Monte Carlo simulation versus semiempirical calculation of autoabsorption factors for semiconductor detector calibration in complex geometries, *Progress in Nuclear Energy* **24**, 327–336 (1990).

[13] H. Zhang and S. X. Chen, Concentration Inequalities for Statistical Inference, *Communications in Mathematical Research* **37** (1), 1-85 (2021).

[14] N.M. Murphy, L. León Vintró, C.I. Burbidge, L. Currivan, An automated programme for the optimisation of HPGe detector parameters using an evolutionary algorithm with GESPECOR, *Applied Radiation and Isotopes* **156**, 108883 (2020).